Investigation of the Influence of Solute-Solvent Interactions on the Vibrational Energy Relaxation Dynamics of Large Molecules in Liquids

Pigliucci, Anatolio; Duvanel, Guillaume; Lawson Daku, Latevi Max; Vauthey, Eric

Investigation of the Influence of Solute−Solvent Interactions on the Vibrational Energy Relaxation Dynamics of Large Molecules in Liquids

Anatolio Pigliucci,[†] Guillaume Duvanel, Latévi Max Lawson Daku, and Eric Vauthey*

Department of Physical Chemistry, University of Geneva, 30 quai Ernest-Ansermet, CH-1211 Genève 4, Switzerland

Received: December 29, 2006; In Final Form: March 5, 2007

The influence of solute−solvent interactions on the vibrational energy relaxation dynamics of perylene and substituted perylenes in the first singlet excited-state upon excitation with moderate (<0.4 eV) excess energy has been investigated by monitoring the early narrowing of their fluorescence spectrum. This narrowing was found to occur on timescales ranging from a few hundreds of femtoseconds to a few picoseconds. Other processes, such as a partial decay of the fluorescence anisotropy and the damping of a low-frequency oscillation due to the propagation of a vibrational wavepacket, were found to take place on a very similar time scale. No significant relationship between the strength of nonspecific solute−solvent interactions and the vibrational energy relaxation dynamics of the solutes could be evidenced. On the other hand, in alcohols the spectral narrowing is faster with a solute having H-bonding sites, indicating that this specific interaction tends to favor vibrational energy relaxation. No relationship between the dynamics of spectral narrowing and macroscopic solvent properties, such as the thermal diffusivity, could be found. On the other hand, a correlation between this narrowing dynamics and the number of low-frequency modes of the solvent molecules was evidenced. All these observations cannot be discussed with a model where vibrational energy relaxation occurs via two consecutive and dynamically well-separated steps, namely ultrafast intramolecular vibrational redistribution followed by slower vibrational cooling. On the contrary, the results indicate that both intra- and intermolecular vibrational energy redistribution processes are closely entangled and occur, at least partially, on similar timescales.

Introduction

The transformation of excess excitation energy into heat is a well-known phenomenon in condensed phase photochemistry and photophysics. Indeed, because vibrational energy relaxation (VER) is ultrafast and thus very efficient, the quantum yield and the outcome of most organic photochemical processes are independent of the excitation wavelength, as stated by the rules of Kasha and Valivov.[1] Nevertheless, several photoinduced processes, such as cis−trans isomerization,[2] proton,[3,4] and electron transfer,[5,6] can occur on timescales that are comparable to those of VER. Therefore, the dynamics of these processes might depend on the initial preparation of the excited state. However, to exploit such "non-Kasha" photochemistry, a deep knowledge and understanding of all the steps involved in the relaxation to thermal equilibrium of an electronically excited molecule are first required. This is one of the reasons why VER has been intensively investigated over the past years, both theoretically and experimentally.[7−14]

VER in the condensed phase is usually discussed in terms of two steps, namely intramolecular vibrational energy redistribution (IVR) and vibrational cooling (VC). After excitation of a vibronic transition, the vibrational energy of the molecule is concentrated in Franck−Condon active modes and the excited-state population forms a microcanonical ensemble. Upon IVR, this vibrational energy is redistributed among the other vibrational modes. After this process, which is mainly induced by anharmonic coupling, the excited-state population forms a canonical ensemble and thus a molecular temperature can be defined. Depending on the excess excitation energy and on the size of the molecule, this temperature can be substantially larger than that of the environment and therefore the hot molecule cools down by intermolecular energy transfer. This process has been often discussed theoretically within the isolated binary collision model, where the total energy transfer rate is assumed to be proportional to the solute−solvent collision frequency.[7] Other theoretical models, based on time-dependent perturbation theory have also been proposed.[8,15] The subsequent transport of energy within the solvent has been treated as a classical heat conduction process.[10]

In the gas phase, where it has been mostly studied,[12] IVR of high-frequency modes has been shown to occur via sequential steps: the energy first flows through doorway states from which it is further redistributed into dense bath states. IVR in small molecules takes place within a few tens to hundreds of picoseconds.[12] It has been recently shown that IVR of small molecules in solution is not complete; namely, intermolecular energy transfer to the surrounding occurs before states involving weakly coupled intramolecular vibrational modes are populated.[13] In this case, IVR and VC cannot be differentiated by their timescales. The situation is apparently different for larger molecules in solutions, where IVR and VC have been reported to take place on relatively well-separated timescales. Indeed, for electronically excited molecules IVR times ranging from 10 fs to a few hundreds of femtoseconds[9,11,16,17] and VC times

* Corresponding author. E-mail: eric.vauthey@chiphy.unige.ch.
[†] Present address: Max-Planck-Institut für Quantenoptik, D-85748 Garching, Germany.

10.1021/jp069010y CCC: $37.00
Published on Web 06/26/2007

CHART 1

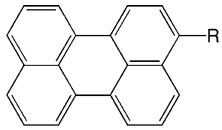

Pe: R=H
PeCN: R=CN
PeOH: R=CH_2OH

between about one and several tens of picoseconds,[16,18−21] can be found in the literature.

The solvent dependence of VC has been the object of several investigations. Sukowski et al. found that the energy transfer to the surrounding from hot azulene in the S_0 state is less efficient in solvents with large molecular mass.[10] This effect was explained by the smaller fraction of translational energy carried away from azulene by a heavier solvent molecule upon collision. Hamaguchi and co-workers have studied the VC dynamics of trans-stilbene in a large variety of solvents, namely, *n*-alkanes, alcohols, and others using time-resolved resonance Raman spectroscopy and found a linear correlation between the VC rate constant and the thermal diffusivity of the solvent.[20,22] This dependence was ascribed to the dissipation of heat from the few solvent molecules surrounding the hot solute. A similar dependence on the thermal diffusivity has been reported more recently with a merocyanine dye in polar solvents.[23] Kovalenko et al. have examined the effect of solute−solvent interactions on the VC dynamics of stilbene and highly polar nitroanilines in protic and nonprotic polar solvents.[16] The VC dynamics of polar solutes was biexponential while that of stilbene was monoexponential. This was explained by a stronger solute−solvent interaction in the former case, which leads to local heating effects (i.e., the heating of the more strongly coupled solvent molecules). For all three solutes, the VC was found to be slower in aprotic solvents. Moreover, in aprotic solvents the measured VC of polar solutes was faster in the more polar solvents. The latter polarity dependence was not observed with the nonpolar stilbene. The solutes used in this investigation were chemically very dissimilar, and therefore the difference in VC for the various solutes in a given solvent cannot be only ascribed to the effects of solute−solvent interactions, but could also be due to differences in their intramolecular dynamics.

We report here on our investigation of the dynamics of VER of perylene (Pe) and substituted perylenes in nonpolar, polar, protic, and aprotic solvents, using femtosecond-resolved fluorescence spectroscopy. As shown in Chart 1, these perylenes are structurally very similar and should thus be well suited to explore the influence of solute−solvent interactions on the VER dynamics. The effect of dipole−dipole interaction can in principle be studied by comparing the VER dynamics of perylene and cyanoperylene in polar solvents. Moreover, methanolperylene allows the effect of H-bonding to be examined.

The VER dynamics of Pe has already been investigated in both gas and condensed phases. The time scale of IVR in a supersonic jet was determined to be of the order of 5−100 ps, depending on the excess excitation energy.[24−26] Rullière and co-workers have measured the population dynamics of Pe in the S_1 state after excitation of the $S_0 \rightarrow S_{3,4}$ transitions in solvents of various polarities and viscosities.[27] A rising component with a time constant of the order of 30 ps, close to the time-resolution of the experiment, was observed and attributed to VER. No significant solvent dependence was detected. More recently, Blanchard et al. have measured the fluorescence dynamics of Pe in *n*-alkanes of different length using stimulated emission spectroscopy with 10 ps resolution.[28] The rise time of the fluorescence in a wavelength region corresponding to S_1 ($v = 0$) $\rightarrow$ S_0 ($v \neq 0$) emission was attributed to the lifetime of the vibrational excited state. Time constants ranging from less than 10 to about 400 ps were reported, but no relationship between alkane length and VER time constant was found. This was attributed to the occurrence of "short range order" of some alkanes around Pe. Finally, a study of VER dynamics of Pe in various ketones using femtosecond fluorescence up-conversion has been published very recently.[29] Three VER timescales, around 150 fs, 800 fs, and 3 ps, were reported with the first two assigned to IVR and the last to VC. In this case again, no relationship between the VC time constant and the chain-length of the ketones could be identified.

Experimental

Samples. Perylene (Pe) was recrystallized in benzene before use. Perylene-d_{12} (PeD) and 3-cyanoperylene (PeCN) were synthesized according to literature[30,31] and were purified by column chromatography. 3-Methanolperylene (PeOH) was purchased from MicroChemistry Ltd. and was used without further purification. The solvents acetonitrile (ACN), perdeuterated acetonitrile (ACNd), dimethylsulfoxide (DMSO), perdeuterated dimethylsulfoxide (DMSOd), methanol (MeOH), 2-propanol (PrOH), octanol (OcOH), toluene (TOL), perdeuterated toluene (TOLd), and cyclohexane (CHX) were of the highest commercially available purity and were used as received. The perdeurated solvents were from Cambridge Isotope Laboratories Ltd.

Steady-State Measurements. Absorption spectra were recorded on a Cary 50 spectrophotometer, while fluorescence and excitation spectra were measured on a Cary Eclipse fluorimeter in a 1 cm quartz cell.

For gas-phase measurements of Pe fluorescence, a small crystal was placed in a vacuum-sealed quartz cell. The latter was then positioned in a metallic housing in contact with a heating plate. The sample was excited at 375 nm, and the fluorescence was detected with a CCD camera (Oriel Intaspec IV)) after dispersion with a 250 mm spectrograph (Oriel Multispec 257).

Time-Resolved Fluorescence. The fluorescence up-conversion setup used for the measurements was basically the same as that described earlier.[32] Excitation was performed at 400 nm using the frequency-doubled or tripled output of a Kerr lens mode-locked Ti:sapphire laser (Tsunami, Spectra-Physics) operating at 82 MHz. The sample solutions were placed in a rotating cell of 0.4 mm optical path length. The concentration of the chromophores was adjusted to obtain an absorbance of 0.1−0.15 on 0.4 mm at the excitation wavelength and thus did not exceed 3×10^{-4} M. The pump intensity on the sample was kept below 10^{12} photons cm^{-2} $pulse^{-1}$ to avoid the population of upper excited states upon two-photon absorption. The polarization of the pump beam was at magic angle relative to that of the gate pulses at 800 nm except for fluorescence anisotropy measurements. The fluorescence time profiles were measured at 5 to 10 different wavelengths throughout the fluorescence spectrum of the chromophores and over two different timescales. The full width at half-maximum of the instrument response function was around 210 fs.

Data Analysis. The fluorescence time profiles measured at different wavelengths and timescales were analyzed globally by iterative reconvolution of the instrument response function with a sum of exponentials using a nonlinear least-square fitting procedure (MATLAB, The MathWorks, Inc.).

Computation. Density functional theory[33,34] calculations were carried out with the Gaussian program package[35] to determine

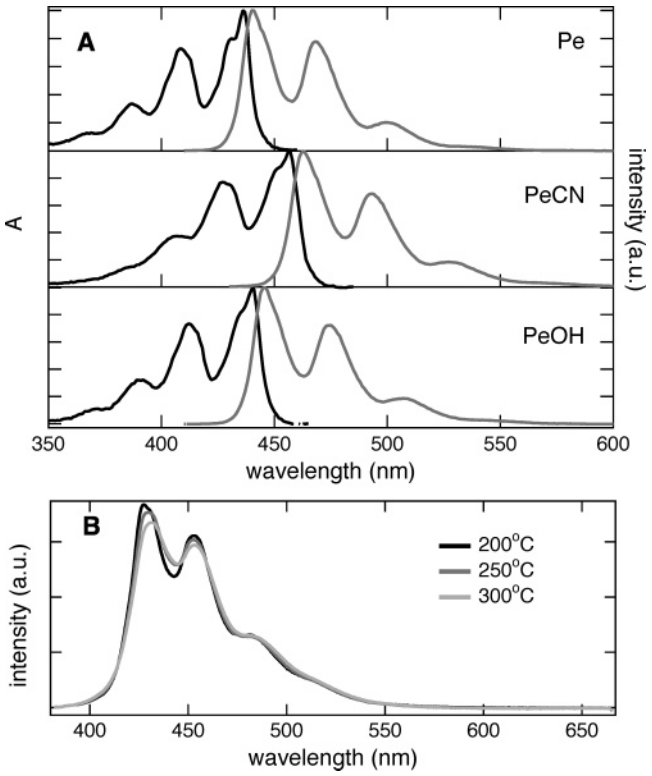

Figure 1. (A) Absorption and fluorescence spectra of the chromophores in CHX. (B) Gas-phase fluorescence spectra of Pe recorded at different temperatures and normalized to the same area.

the geometries and the vibrational frequencies of the chromophores and of the different solvent molecules in the electronic ground state. The calculations were done with the PBE exchange-correlation functional,[36] and all atoms were described with the 6-311+G** basis set of triple-ζ polarized quality and augmented with a set of diffused functions for the heavy atoms.[37,38] The implemented "ultrafine" integration grid was employed in all cases and the geometry optimizations were performed using the "tight" convergence criterion.

Results

Steady-State Spectra. The absorption and fluorescence spectra of Pe, PeCN, and PeOH in CHX are illustrated in Figure 1A. The spectra of PeD are almost identical to those of Pe. In the six other solvents investigated (ACN, DMSO, MeOH, PrOH, OcOH, TOL), the spectra are very similar to those in CHX. For Pe and PeD, only a small red shift of both absorption and emission bands is noticed upon going from low (ACN, MeOH) to higher refractive index solvents (DMSO, TOL). A plot of the absorption and fluorescence maxima in energy units versus the function, $f(n^2) = 2(n^2 - 1)/(2n^2 + 1)$ where n is the refractive index, results in reasonably straight lines (Figure S1 in Supporting Information), indicating that the solvatochromism of Pe and PeD is dominated by dispersion interactions.[39] The S_1 energy of Pe and PeD, calculated from the absorption and emission maxima, varies from 2.79 eV in DMSO to 2.84 eV in MeOH.

A qualitatively similar solvatochromism was measured with PeOH, for which the S_1 energy increases from 2.76 to 2.81 eV in the same two solvents. The calculated dipole moment of PeOH in the ground state has been reported to amount to about 2 D.[40] The good correlation of the transition energy with $f(n^2)$ and the absence of correlation with the polarity function $f(\epsilon_0) = 2(\epsilon_0 - 1)/(2\epsilon_0 + 1)$, where ϵ_0 is the static dielectric constant, indicates that the electric dipole moment of PeOH does essentially not change upon excitation and that the S_0-S_1 transition is almost totally localized on the perylene moiety and thus does not involve the hydroxymethyl substituent. This conclusion is further supported by the total insensitivity of both absorption and emission spectra of PeOH to the H-bonding property of the solvents. This shows that in H-bonding solvents, the stabilization energy is the same in both S_0 and S_1 states, confirming that the electronic distribution on the hydroxymethyl substituent remains unchanged upon excitation.

Contrary to the other chromophores, the solvatochromism of PeCN exhibits additionally a slight dependence on the polarity function $f(\epsilon_0)$ with the S_1 energy varying from 2.65 eV in ACN to 2.76 eV in CHX. A plot of the fluorescence maximum in energy units as a function of $f(\epsilon_0) - f(n^2)$ exhibits a rather good linear relationship with a slope of -1600 cm^{-1} once the values in both DMSO and TOL, which have a considerably higher refractive index, have been eliminated (Figure S2 in Supporting Information). A calculated dipole moment of 4.2 D has been reported for PeCN in the ground state.[40] The insertion of this value and the slope of the solvatochromic plot in the usual equation for the fluorescence solvatochromism due to dipole−dipole interaction[39] yield an electric dipole moment of about 6 D for PeCN in the S_1 state.

Figure 1B shows the fluorescence spectrum of Pe in the gas phase recorded at different temperatures and normalized to the same area. The spectrum becomes broader and structureless as the temperature increases. The fluorescence intensity at the wings of the spectrum increases with temperature, while that at the band maxima decreases. A qualitatively similar temperature effect has been reported for azulene.[41]

Early Spectral Narrowing. Figure 2A shows early time profiles of Pe fluorescence in ACN upon 400 nm excitation. At wavelengths below 430 nm and above 500 nm (i.e., on the edges of the fluorescence band) the intensity decays during the first few picoseconds and then remains constant over the time window of the experiment. Between these two wavelengths, the early fluorescence exhibits a prompt rise followed by a slower growth to a constant intensity. Measurements with a larger time window show that this intensity decays on the nanosecond time scale in agreement with a fluorescence lifetime of Pe of the order of 4.4 ns in aerated solutions.[40]

These profiles have been used to reconstruct the time-resolved fluorescence spectra depicted on a logarithmic scale in Figure 2B, which reveals that the early fluorescence dynamics corresponds to a narrowing of the emission spectrum taking place during the first few picoseconds after excitation. The qualitatively similar narrowing illustrated in Figure 1B upon decreasing temperature confirms that this effect is related to VER, the distinction between IVR and VC being not made at the present stage. As the solvatochromism of Pe is dominated by dispersion forces, contribution of solvent relaxation to the observed spectral dynamics can be safely excluded.

The fluorescence time profiles could be analyzed globally using the sum of two exponentials as trial function. The time constants obtained with Pe in ACN amount to 0.5 and 4.6 ps. As the magnitude of this early fluorescence dynamics is relatively small, especially at wavelengths located around the center of the spectrum, the uncertainty on the relative amplitudes associated with these two time constants is quite large. On the wings of the spectrum, the amplitude of the fast and slow components is of the order of 0.4 ± 0.2 and 0.6 ± 0.2, respectively. A similar biphasic spectral narrowing has been measured with Pe in all the other solvents except TOL, where the early dy-

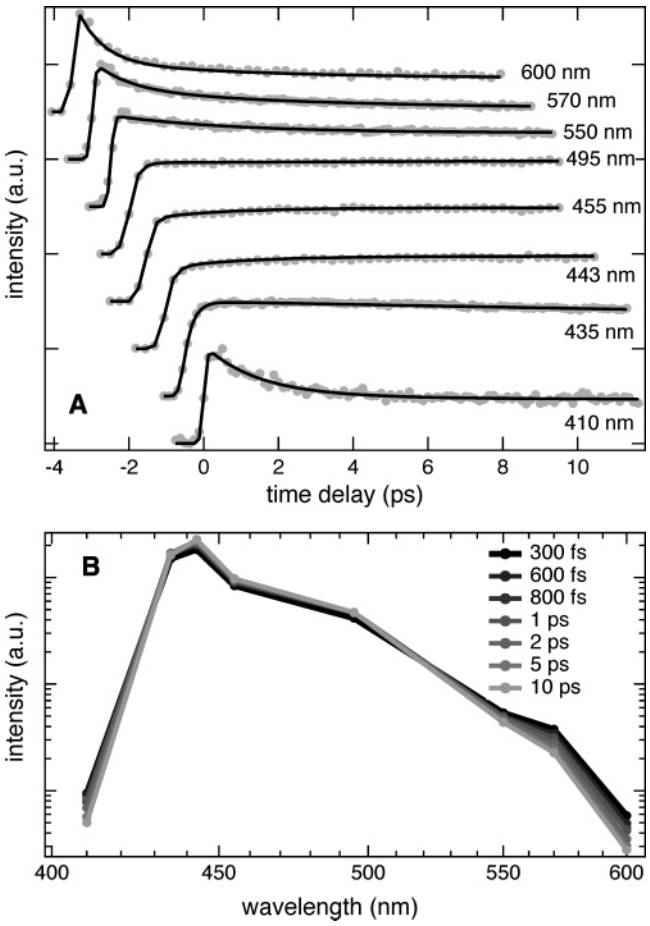

Figure 2. (A) Time profiles of the fluorescence of Pe in ACN measured at different wavelengths. (B) Reconstructed time-resolved fluorescence spectra of Pe in ACN.

TABLE 1: Time Constants (in ps) Associated with the Early Narrowing of the Fluorescence Spectrum of the Chromophores upon 400 nm Excitation Obtained from a Global Fit Using a Mono- or a Biexponential Function (Limit of Error: ±10%)[a]

	Pe			PeD			PeCN	PeOH
solvent	τ_{sn1}	τ_{sn2}	$<\tau_{sn}>$	τ_{sn1}	τ_{sn2}	$<\tau_{sn}>$	τ_{sn}	τ_{sn}
ACN	0.5	4.6	2.9	0.9	6.5	3.7	0.7	0.7
ACNd				0.5	4.5	2.5		
DMSO	0.2	1.3	0.9	0.4	5.4	3.1	0.6	0.8
DMSOd				1.6		1.6		
MeOH	0.6	4.5	2.6	2.0		2.0	2.1	1.0
PrOH	0.4	2.6	1.7	1.4		1.4	1.5	1.2
OcOH	0.2	3.0	2.0	1.5		1.5	1.3	1.1
TOL	2.4		2.4	1.8		1.8	1.1	1.1
TOLd	2.7		2.7	1.9		1.9		
CHX	0.4	4.1	2.8	2.2		2.2	1.2	1.4

[a] For Pe and PeD, lifetimes from single-exponential fits are listed in the τ_{sn1} and $<\tau_{sn}>$ columns.

namics could be reproduced with a single-exponential function. All of the resulting time constants, τ_{sn}, are listed in Table 1.

Such measurements have also been carried out with PeD, PeCN, and PeOH in the same series of solvents and the results are summarized in Table 1. It can be seen that, except for PeD in ACN and DMSO, the spectral narrowing is monophasic. In addition to the spectral narrowing, a dynamic Stokes shift of the fluorescence spectrum related to solvent relaxation could have been expected with PeCN, which exhibits some weak but significant solvatochromism due to dipole−dipole interaction. The signature of such an effect is the presence of decaying components at short wavelengths, as observed, and of rising components at long wavelengths. Given that such rise at long wavelengths was not observed and that the time profiles could be analyzed globally with a single-exponential function, it can be concluded that the contribution of solvent relaxation to the early fluorescence of PeCN is substantially smaller than that of VER. This conclusion is further supported by the fact that a significant part of solvation dynamics of alcohols like PrOH and OcOH is known to involve much longer time constants than those found here.[42] Moreover, it should be noted that the fluorophores used for dynamic Stokes shift measurements are characterized by a much larger dipole moment difference between ground and excited states than that found for PeCN.[43,44]

Vibrational Wavepacket. In addition to the early spectral narrowing due to VER, a periodic oscillation of the fluorescence intensity was observed (see Figure 3). This oscillation is due to the propagation of a vibrational wavepacket caused by the impulsive excitation of a low-frequency Franck−Condon active mode. With Pe, this oscillation has a weak amplitude, requiring measurements with a high signal-to-noise (S/N) ratio and is only observed within a narrow wavelength range, typically around 475 nm. In TOL and TOLd, the wavepacket can also be detected over a broader range, namely, between 440 and about 500 nm. On the other hand, no oscillation could be seen in DMSO. With PeD, the oscillation was found in all solvents and over a much broader spectral range, typically between 410 and 550 nm (Figure 3A). With PeCN, no intensity modulation by a vibrational wavepacket could be found in the first place. However, measurements in CHX with a very high S/N ratio allowed a weak modulation to be detected (Figure 3B). In ACN, the oscillation amplitude was too small for any reliable information to be extracted. Very high S/N ratio measurements for detecting wavepacket oscillation were not performed with PeOH.

The wavepacket contribution was analyzed in two different ways. In the first, the time profiles were analyzed as described above with a trial function consisting of one or two exponentials but with the additional function

$$f(t) = A_{wp} \cos(\omega_{wp} t - \phi) \exp(-t/\tau_{wp}) \qquad (1)$$

where A_{wp} is the amplitude of the oscillation, ω_{wp} is its angular frequency, τ_{wp} is its damping time, and ϕ is a phase factor. The resulting best-fits with PeD are shown in Figure 3A. In the second, the time profiles were analyzed without introducing eq 1 in the trial function. The oscillating part of the signal was then isolated by subtracting the calculated time profile from the measured one before being Fourier transformed (Figure 4). The oscillation amplitude with Pe was too small to obtain a reliable value of τ_{wp}. On the other hand, both analyses resulted in a very similar oscillation frequency. The latter is essentially independent of the solvent and corresponds to a frequency $\bar{\nu}_{wp} = \omega_{wp}/2\pi c$ between 74 and 76 cm^{-1}.

With PeD, the frequency is also independent of wavelength and solvent and amounts to $\bar{\nu}_{wp} = 65 \pm 1$ cm^{-1}. However, a decrease of the oscillation amplitude with increasing wavelength was noticed. For example, A_{wp} in ACN relative to the total fluorescence intensity varies from 5 to 3% by going from 420 to 530 nm. Moreover, in a given solvent τ_{wp} decreases somewhat with increasing wavelength. In ACN, τ_{wp} decreases from 2.2 ± 0.5 ps at 420 nm to 1.6 ± 0.4 ps at 530 nm. The average τ_{wp} values obtained from the fit with eq 1 to the time profiles recorded around 420, 480, and 530 nm are listed in Table 2.

The frequency found with PeCN in CHX amounts to $\bar{\nu}_{wp} =$

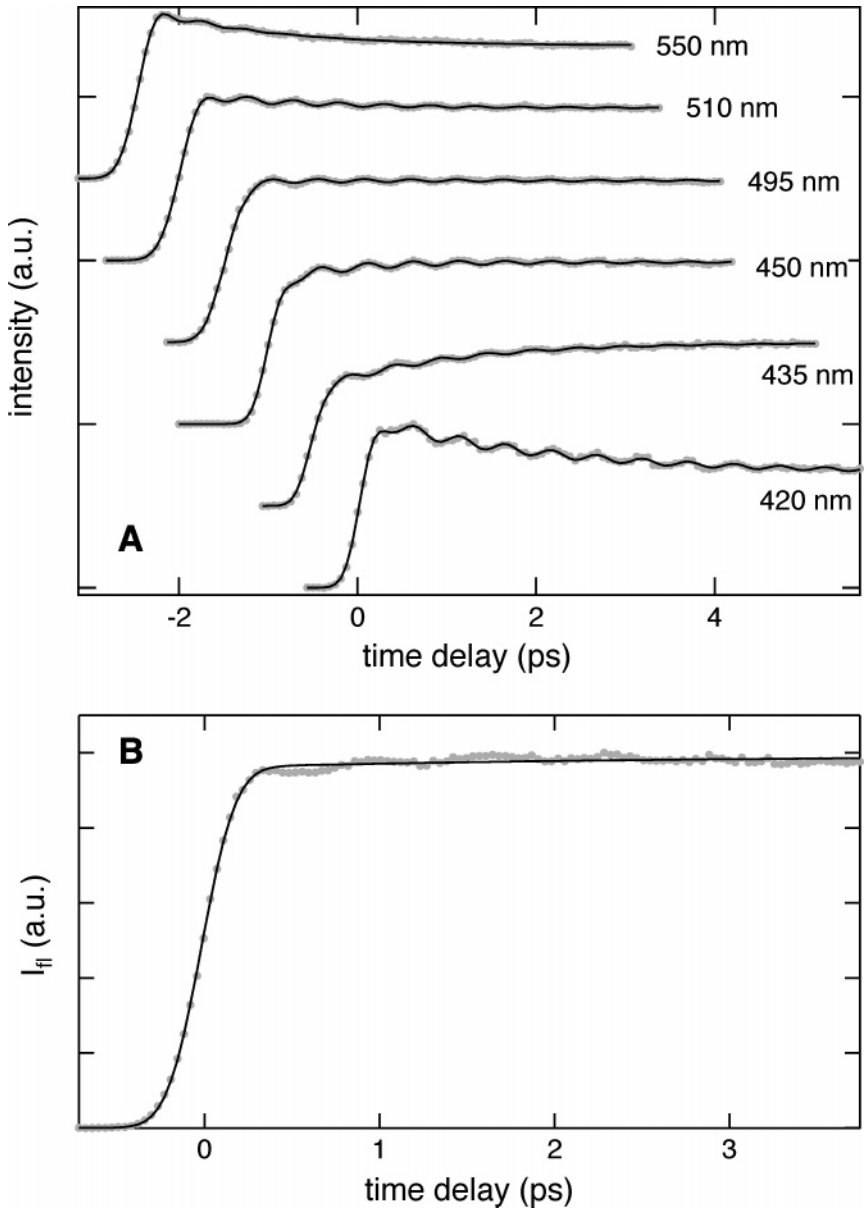

Figure 3. Time profiles of the fluorescence of (A) PeD in TOL at different wavelengths and (B) PeCN in CHX at 485 nm.

47 ± 2 cm^{-1}. The dependence of this value on wavelength and solvent was not investigated.

Fluorescence Anisotropy. The early dynamics of the fluorescence polarization anisotropy, *r*, has also been measured with Pe, PeD, and PeCN in a few solvents. It was calculated as $r(t) = (I_{||}(t) - I_{\perp}(t))/(I_{||}(t) + 2I_{\perp}(t))$, where $I_{||}(t)$ and $I_{\perp}(t)$ are the time profiles of the fluorescence polarized in directions parallel and perpendicular to that of the excitation light, respectively. Figure 5A shows the decay of the fluorescence anisotropy recorded with PeCN in ACN at 510 nm. This decay can be properly reproduced using a single-exponential function with a time constant of 20 ps. This value compares well with that of 19 ps found from optically heterodyned polarization measurements at 400 nm and ascribed to the reorientational motion of PeCN in the electronic ground state.[40] The initial anisotropy, $r(0)$, is of the order of 0.3 (i.e., substantially smaller than that of 0.4 expected for a fluorescence transition dipole moment parallel to that for absorption). A similar low initial anisotropy value has been reported with Pe in various classes of solvents[45−48] and has been explained in terms of a rapid libration of Pe[47] and vibronic coupling.[49]

Figure 5B shows the initial anisotropy dynamics measured at 455 nm, namely at the blue onset of the fluorescence band of PeCN. At this wavelength, the anisotropy decays from an initial value of 0.4 to about 0.3 with a time constant of 700 fs. The residual anisotropy goes then to zero with a 20 ps time constant. A similar biphasic decay of *r* has also been measured in DMSO at 445 nm. The results are summarized in Table 3 together with those obtained with Pe and PeD in the same solvent. With both of these chromophores, the measured initial anisotropy also exhibits a decrease upon increasing wavelength.

This initial ultrafast decay is clearly too fast to originate from diffusional reorientation and occurs on a similar time scale as that of spectral narrowing (see Table 1). As discussed in the next section, it is thus most probably related to VER.

Discussion

As discussed in the introduction, VER processes taking place on the picosecond time scale have in most cases been ascribed to VC,[16,18−21] and their solvent dependence, in some cases,[20,22,23] has been discussed in terms of thermal bulk properties of the solvents. We will show in the following that such correlation

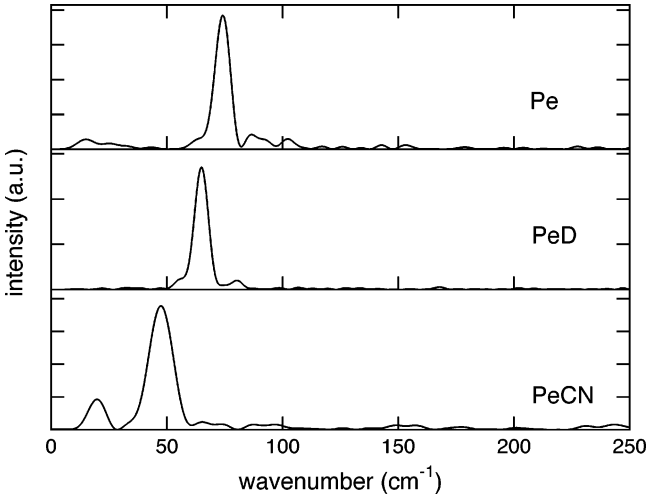

Figure 4. Fourier transforms of the oscillating part of the fluorescence time profiles measured at 465 nm with Pe and PeD in TOL and at 485 nm with PeCN in CHX.

TABLE 2: Damping Times of the Vibrational Wavepacket Obtained by Averaging the Values Resulting from the Analysis of the Time Profiles of PeD around 420, 480, and 530 nm (Limit of Error: ±0.25 ps)

solvent	τ_{wp} (ps)
ACN	1.8
DMSO	1.3
MeOH	2.15
PrOH	1.8
OcOH	2.05
TOL	2.4
CHX	2.3

between the VER timescales reported here and macroscopic solvent properties, such as thermal diffusivity, cannot be evidenced. In other words, the dynamic features found here cannot be described as the cooling of a hot molecule upon interaction with a bath consisting of a quasi-continuum of states. On the contrary, the results can be reasonably well rationalized within a model where both intra- and intermolecular vibrational energy redistribution occur in parallel and thus where the density of vibrational states of the solvent molecules plays a major role.

The amount of excess excitation energy that is redistributed in vibrational modes, E_E, can be estimated by considering the energy of the S_1 state of the various chromophores in CHX, which is an apolar solvent with a refractive index between those of MeOH and TOL. With 400 nm excitation, this energy amounts to about 0.3 eV for Pe, PeD, and PeOH and to 0.4 eV for PeCN. If this excess energy is only dissipated into intramolecular modes, the resulting vibrational temperature, T, can be calculated with the following equation[50]

$$E_E = \sum_{i=1}^{3N-6} \frac{h\upsilon_{c,i}}{\exp(h\upsilon_{c,i}/k_B T) - 1} \qquad (2)$$

where N is the number of atoms of the chromophore, $\upsilon_{c,i}$ is the frequency of the vibrational mode i, and k_B is the Boltzmann constant. The vibrational frequencies of Pe, PeD, PeCN, and PeOH in the electronic ground state have been determined from quantum chemical calculations. The validity of the calculated frequencies has been checked by comparison with those already published for Pe.[51,52] In principle, the vibration frequencies of the chromophores in the first singlet-excited state should be used here. However, their calculation is much more demanding than for the molecules in the ground state. As these frequencies can be expected to be shifted by an amount going from a few wavenumbers to a few tens of wavenumbers relatively to those of the ground state,[52] the resulting temperatures should not differ very significantly.

This equation predicts a vibrational temperature after IVR of 400 K for Pe. For PeD and PeOH, the temperature is slightly smaller (i.e., 390 K) because of a downshift of the vibration frequencies for PeD and of the existence of 12 additional normal modes in PeOH. A higher temperature is calculated for PeCN (i.e., 420 K) because of the larger excess excitation energy.

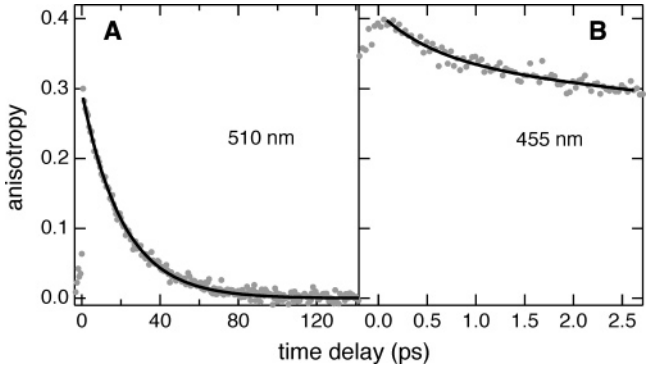

Figure 5. Decays of the fluorescence anisotropy measured with PeCN in ACN at two different wavelengths.

TABLE 3: Parameters Obtained from the Analysis of the Early Fluorescence Anisotropy Decay upon 400 nm Excitation: Anisotropy at Time Zero, r_0, Time Constant, τ_{r1}, and Amplitude, r_1, of the Fast Decaying Component

chromophore	solvent	λ (nm)	r_0	τ_{r1} (ps)	r_1
Pe	DMSO	420	0.39	0.3	0.05
		570	0.35		
PeD	DMSO	420	0.39	0.2	0.07
		570	0.30		0
PeCN	ACN	445	0.40	0.7	0.10
		610	0.27		0
	DMSO	445	0.40	0.5	0.05

Relationship between Spectral Narrowing and Bulk Solvent Properties. The data listed in Table 1 indicate that the dynamics of the spectral narrowing does not depend very strongly on both the solute and the solvent. Indeed, if we consider average values for the cases where the narrowing is biphasic, the measured time constants ranges from 0.6 to 3.5 ps.

A first difference between the spectral narrowing dynamics measured here is that it is biphasic with Pe, except in TOL, while is it characterized by a single time constant with PeOH and PeCN. The origin of such a difference is not clear. Similar biphasic dynamics have already been reported in the literature.[16,23,29] Kovalenko et al. have observed it in polar solvents with a very polar solute in the hot ground state after ultrafast internal conversion from the initially populated S_1 state.[16] This effect was ascribed to a strong solute−solvent coupling that leads to a local heating effect, the fast component reflecting solute−solvent energy transfer and the slow one the cooling of the first solvent shell by the bulk solvent. In this study, the amount of vibrational energy to be dissipated was exceeding 2 eV. On the other hand, Benniston et al. have ascribed the fast part of the observed spectral dynamics to VC and the slower part, which was viscosity dependent, to conformational changes.[23] More recently, Kiba et al. have found three different time constants for the spectral narrowing of Pe fluorescence in various

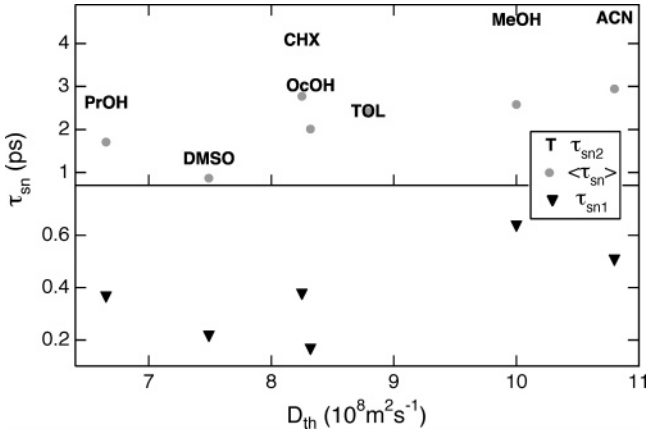

Figure 6. Time constants associated with the spectral narrowing measured with Pe as of function of the thermal diffusivity of the solvents (D_{th}values taken from refs 20, 23, 53−56).

ketones.[29] The two smaller time constants, around 200 and 800 fs, were ascribed to IVR, while the longer one was assigned to VC.

A local heating effect seems not to be at the origin of the biphasic dynamics measured here, first because a rather weak solute−solvent coupling can be expected with the nonpolar Pe, and second because the excess energy upon 400 nm excitation is certainly not high enough to result in a very large temperature rise of the first solvent layer.

As mentioned in the introduction, VC dynamics has been reported by several groups to be strongly correlated with the thermal diffusivity of the solvent, D_{th}.[10,20,22] The existence of such a correlation has been tested with both time constants measured with Pe as well with their average values. Figure 6 shows that the smaller time constant, τ_{sn1}, is essentially independent of D_{th}, while the larger time constant, τ_{sn2}, and the average time constant, $<\tau_{sn}>$, seem to increase with increasing thermal diffusivity. This apparent trend is exactly opposite to the dependences reported in the literature in which the VC time constant was decreasing with increasing D_{th}, as one would expect for a cooling process. Consequently, the trend shown in Figure 6 is most probably fortuitous. Moreover, it should be noted that this correlation is not present with PeCN and PeOH. The existence of a correlation between the τ_{sn} values and other bulk properties of the solvents such as the thermal conductivity, the heat capacity, the density, and the viscosity was also tested. No clear relationship could be found with any of the chromophores.

Relationship between Spectral Narrowing and Solute−Solvent Interactions. One aim of the present work was to look for a connection between solute−solvent interactions and VER dynamics. With Pe, dispersion is the dominating interaction and thus no relationship between the VER dynamics and the dielectric constant or the H-bonding ability of the solvents is anticipated, which is in agreement with the measurements. It is interesting to note that in TOL, where $\pi-\pi$ interactions are probably the largest, the spectral narrowing is monophasic contrary to the other solvents. Perdeuteration of Pe should in principle not significantly influence the solute−solvent interaction. However, isotopic substitution results in substantial changes of the dynamics, as the latter becomes monophasic in most solvents except in ACN and DMSO. Moreover, in these two solvents both τ_{sn1} and τ_{sn2} are substantially larger with PeD than with Pe. This is a clear indication that the biphasic nature of the narrowing observed here does not originate from a local heating effect. If this were the case, τ_{sn2} should not be influenced by Pe perdeuteration. The biphasic dynamics might be unrelated to the presence of two distinct time scales of similar amplitudes but could rather originate from a distribution of time constants with a Gaussian distribution of amplitudes.[57,58] This might reflect the presence of many different VER pathways. In some cases, this distribution could be narrow enough to give rise to apparent monophasic dynamics.

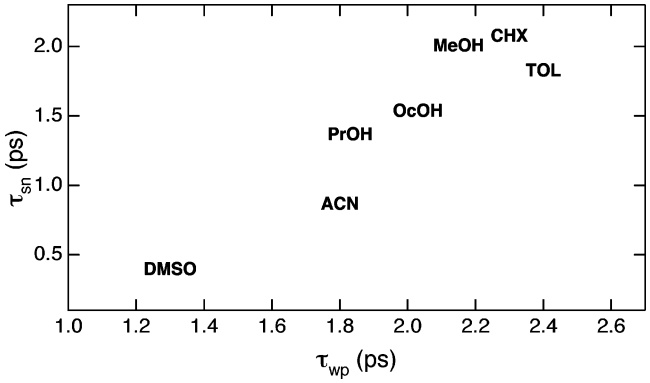

Figure 7. Time constant associated with the spectral narrowing of PeD as a function of the lifetime of the vibrational wavepacket.

Contrary to Pe and PeD, dipole−dipole interaction should additionally be operative with PeCN in polar solvents. A look at Table 1 shows that τ_{sn} with PeCN is always smaller than $<\tau_{sn}>$ with PeD. However, the magnitude of this effect is apparently not linked to the polarity of the solvent and, hence, to the strength of the dipole−dipole interaction. Indeed, the difference in τ_{sn} by going from PeD to PeCN is small in MeOH and quite large in CHX and TOL. This difference must thus be rather connected with changes in the vibrational energy levels by going from PeD to PeCN. This conclusion also agrees with the dissimilarities observed between Pe and PeD.

Finally, the spectral-narrowing dynamics of PeOH and PeCN are comparable except in alcohols, where it is noticeably faster with PeOH. It seems reasonable to ascribe this effect to the occurrence of H-bonding. The difference between PeOH and PeCN grows in the order OcOH, PrOH, and MeOH, which also corresponds to the increase of the Kamlet parameter α, describing the H-bond donating ability of the solvent.[59] The effect of H-bonding on the VER dynamics can be twofold: (1) the H-bound solute−solvent complex can be considered as a supermolecule with a larger number of vibrational degrees of freedom and, as a consequence, with more pathways for intramolecular energy redistribution, and (2) H-bonding connects the chromophore to the whole H-bonding network of the bath and should thus favor intermolecular energy transfer.

Kovalenko et al. have reported a faster VC in protic solvents, but in contrast to our findings, this effect was also measured with non-H-bonding solutes.[16]

Relationship between Spectral Narrowing and Wavepacket Dynamics. As shown in Table 2, the damping time of the vibrational wavepacket, τ_{wp}, measured with PeD depends on the solvent. Interestingly, if only those solvents where spectral narrowing is monophasic are considered, a rather good correlation between τ_{sn} and τ_{wp} can be seen, as illustrated in Figure 7. The wavepackets with the longest lifetime are observed in solvents where the spectral narrowing is the slowest. In ACN and DMSO, where the narrowing is biphasic, the correlation is still very good if only the τ_{sn1} is considered. Although such a correlation could be fortuitous, a relationship between VER and the lifetime of a vibrational wavepacket is physically reasonable. With Pe, this wavepacket is much less pronounced except in TOL where it can be seen at several wavelengths. This

observation is in qualitative agreement with the correlation between τ_{sn} and τ_{wp} found with PeD. In most solvents, the narrowing of Pe fluorescence spectrum is biphasic and τ_{sn1} is very small. Thus a short wavepacket lifetime and a relatively weak modulation amplitude are anticipated. In TOL, the narrowing is monophasic and the associated lifetime is much larger that the τ_{sn1} values in the other solvents. A longer-lived wavepacket and hence a more pronounced oscillation are predicted, which agrees with the observation.

The frequency of this oscillation amounts to about 75 and 65 cm^{-1} for Pe and PeD, respectively. A 95 cm^{-1} mode has been deduced from the fluorescence excitation spectrum of jet-cooled Pe.[24,25] Recent calculations point to a b_{1u} vibrational mode at 86 cm^{-1} for Pe in the S_1 state.[52] From our ground state calculations, this mode is at 90 and 84 cm^{-1} for Pe and PeD, respectively (Table S1 in Supporting Information). However, according to its symmetry this mode should not be excited upon an allowed electronic transition. The first totally symmetric mode of Pe(S_1) is at 345 cm^{-1},[52] while in the S_0 state it is at 348 and 334 cm^{-1} for Pe and PeD, respectively. It is however at too high a frequency to be coherently excited with a 100 fs pump pulse. Several authors[26,52] have suggested that the 95 cm^{-1} band observed in the fluorescence excitation spectrum of jet-cooled Pe is due to an overtone transition of a lower frequency mode at 48 cm^{-1}, assigned to the $1a_{1u}$ mode by Salama and co-workers.[52] This is the lowest frequency mode of Pe and corresponds to the torsional motion of the two naphthalene moieties of Pe about the two single bonds connecting them. As a consequence, the vibrational wavepacket observed with Pe and PeD is probably due the coherent excitation of overtones of this mode, namely $(1a_{1u})^n$ with $n = 2,4,...$ Such overtone transitions are typical for molecules with torsional modes and with a double-well potential either in the S_0 or S_1 states.[60−62] Overtone transitions of the butterfly mode of pentacene have also been invoked to explain its gas-phase fluorescence excitation spectrum.[63] The S_0 potential along the butterfly mode of Pe ($1b_{1u}$ mode at 95 cm^{-1})[52] has been shown to have a very flat minimum, similar to a double-well potential with an extremely low potential energy barrier, while the S_1 potential is almost harmonic.[64] This difference is because Pe in the ground electronic state is not a "true" aromatic hydrocarbon but corresponds rather to two naphthalene moieties connected by two almost single C−C bonds.[26] On the other hand, the aromatic character of Pe is increased in the S_1 state and thus the potential of this state is more harmonic. Because of this structural difference between Pe S_0 and S_1 states, the potentials of these two states along the $1a_{1u}$ mode can also be expected to differ sufficiently to enable overtone excitation.

From our data, the $1a_{1u}$ mode should be at 37.5 and 32.5 cm^{-1} for Pe and PeD in the S_1 state, respectively. These values are close to that of 37 cm^{-1} calculated for Pe in the S_1 state but smaller than that of 48 cm^{-1} reported from jet-cooled Pe.[52] The difference is probably due to the solvent, which can be expected to somehow influence the relatively large amplitude motion associated with this mode. These values are also substantially larger than those calculated for the ground state and amounting to 21 and 19 cm^{-1} for Pe and PeD, respectively. This difference in frequencies is reasonable in view of the structural difference between S_0 and S_1 states discussed just above. Despite this, the decrease of the frequency observed on going from Pe to PeD is reproduced by the calculations. By analogy with Pe and PeD, the 47 cm^{-1} wavepacket oscillation detected with PeCN is assigned to the overtone excitation of its lowest mode, namely the $1a''$ mode. Its frequency in the ground state is predicted to be at 16.5 cm^{-1} (Table S2 in Supporting Information), while our results indicate a frequency around 23 cm^{-1} in the S_1 state.

The damping time of the wavepacket can be expressed as

$$\tau_{wp}^{-1} = \frac{1}{2T_1} + \frac{1}{T_2^*} \quad (3)$$

where T_1 is the population lifetime of the excited vibrational state and T_2^* the pure dephasing time due to the interaction with the environment. Our results do not allow the contribution of each of these processes to the lifetime of the vibrational coherence to be determined. The correlation of τ_{wp} with τ_{sn} indicates that this lifetime reflects VER dynamics. Both T_1 and T_2^* processes could account for such a relationship:

(1) As the wavepacket is associated with the lowest frequency mode, a T_1 process has to occur by energy transfer to the solvent.

2) In a T_2^* process, the dephasing of the coherence is due to collisions with the solvent molecules. Such collisions should also favor intermolecular vibrational energy transfer.

The observation that the wavepacket survives during the spectral narrowing is in contradiction with the picture of well-separated timescales of IVR and VC. Indeed, the existence of a coherent vibrational motion is a sign that the excited-state population is not a canonical ensemble and that a vibrational temperature cannot be really defined. According to eq 2, the molecular temperature after IVR and before VC should rise by about 100 K. In this case, the population of the lowest frequency mode should be strongly affected by IVR. This is clearly not the case, and therefore one can conclude that IVR is not complete before the excited chromophore starts dumping its excess energy into the environment. It is evident that IVR does not proceed on a single time scale. The vibrational energy will be first redistributed in the modes that couple most with the originally excited ones. This first step can be expected to be ultrafast and to occur within a few tens of femtoseconds as reported by Kovalenko et al.[16] However, the vibrational energy redistribution in more weakly coupled modes can be much slower as it is probably the case here for the $1a_{1u}$ mode. It should also be noted that monitoring the shape of an electronic absorption band in liquids is probably not sufficient to judge whether IVR is complete. Such entanglement of intra- and intermolecular VER has been reported by Crim and co-workers by comparing the VER dynamics of CH_3I in the gas phase and in liquids.[13]

Influence of the Vibrational Modes of the Solvent Molecules. A slower IVR implies that the excited states of high-frequency modes may be more populated than assumed for thermal equilibrium. In this case, direct vibrational energy transfer (i.e., V−V transfer) from the solute to solvent modes of similar frequency should be considered.

To evaluate whether the observed solvent dependence of τ_{sn} could be discussed in terms of different matching of the vibrational modes of the solutes and the solvent molecules, their vibrational frequencies have been compared. As the frequencies below 500 cm^{-1} are difficult to access experimentally, values obtained by quantum chemical calculations have been used (see Tables S1−S8 in Supporting Information).

Before considering the frequencies themselves, the existence of a correlation between τ_{sn} and the number of vibrational modes of the solvent molecules, n_s, was examined. Plots of τ_{sn2} and $<\tau_{sn}>$ measured with Pe as a function of n_s (not shown) do not indicate any correlation between these two quantities. On the other hand, Figure 8A reveals that the time constant associated with the fast spectral narrowing component, τ_{sn1}, decreases as

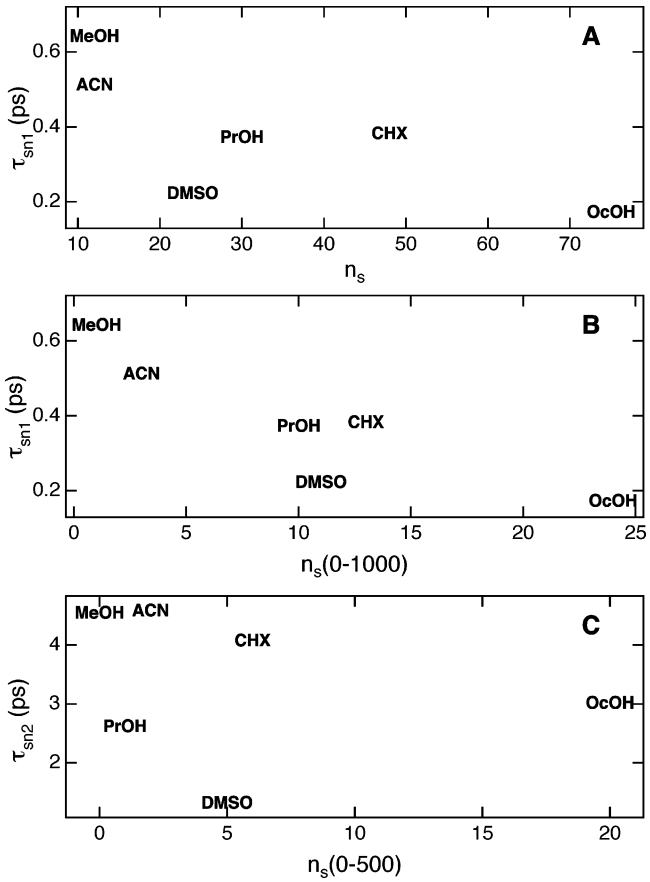

Figure 8. Time constant associated with the fast part of the spectral narrowing of Pe as a function of (A) the number of vibrational modes of the solvent molecules and (B) the number of vibrational modes of the solvent molecules below 1000 cm^{-1}. (C) Time constant associated with the slow part of the spectral narrowing of Pe as a function of the number of vibrational modes of the solvent molecules below 500 cm^{-1}.

n_s increases with the exception of DMSO, which departs markedly from this trend.

In a second step, the number of vibrational modes fulfilling one of the following conditions for single or double quantum transfer was determined for each chromophore and each solvent

$$\bar{\upsilon}_{c,i} = \bar{\upsilon}_{s,j} \pm 5\ \mathrm{cm}^{-1} \quad (4a)$$

$$\bar{\upsilon}_{c,i} = \bar{\upsilon}_{s,j} + \bar{\upsilon}_{s,k} \pm 5\ \mathrm{cm}^{-1} \quad (4b)$$

where $\bar{\upsilon}_c$ and $\bar{\upsilon}_s$ are vibrational frequencies of the chromophore and solvent molecules, respectively. Illumination of Pe at 400 nm (i.e., with about 2400 cm^{-1} excess energy) should excite one high-frequency vibration, such as one of the five totally symmetric modes between 1300 and 1600 cm^{-1} and one or two lower frequency vibrations,[65] including of course the overtone excitation of the $1a_u$ mode. Consequently, only frequencies below 1600 cm^{-1} have been considered. As one could have expected, the number of frequencies fulfilling eq 4a or 4b is proportional to n_s, and therefore the correlation shown in Figure 8A does not really get better if n_s is replaced by the number of modes obeying either eq 4a or 4b. However, a substantial improvement is obtained if only lower frequency modes with $\upsilon_c < 1000$ cm^{-1} and obeying eq 4a are taken into account. The improvement for DMSO is due to the fact that this molecule is characterized by a relatively large number of low-frequency modes with respect to other molecules of similar size, but without a third row atom. In fact, a correlation of the same quality is obtained if the total number of vibrational modes of the solvents with frequencies below 1000 cm^{-1}, n_s (0−1000), is considered independently of eq 4 (see Figure 8B). It appears that the number of vibrational modes fulfilling either eq 4a or 4b in a given frequency range, is roughly proportional to the number of vibrational modes of the solvent molecules in the same frequency range. This can be explained by the relatively large number of normal modes of Pe with frequencies below 1000 cm^{-1}, resulting in a large density of vibrational states. As a consequence, each low frequency solvent mode has a relatively high probability to coincide with a chromophore mode of similar frequency. With smaller chromophores, such correlation would probably be absent.

TABLE 4: Number of Vibrational Modes of the Solvent Molecules within a Given Frequency Range in cm^{-1}

solvent	n_s	n_s (0−1600)	n_s (0−1000)	n_s (0−500)
ACN	12	8	3	2
ACNd	12	8	5	2
DMSO	24	18	11	5
DMSOd	24	18	13	5
MeOH	12	8	1	1
PrOH	30	22	10	6
OcOH	75	57	24	14
TOL	39	30	16	5
TOLd	39	31	21	6
CHX	48	36	13	5

This relationship is particularly important as eq 4 requires the vibrational frequencies of both chromophores and solvents to be known very precisely. Moreover, the $\bar{\upsilon}_c$ values for the chromophores in the first singlet-excited-state should be used. However, knowledge of these frequencies is not required if only the number of vibrational modes of the solvent within a given frequency range is considered. These numbers for a few frequency ranges are listed in Table 4.

The correlation shown in Figure 8B suggests that the fast spectral narrowing observed with Pe is due to V−V transfer occurring from relatively high-frequency modes and taking place in competition to IVR to lower frequency modes. The slower spectral narrowing could be related to a less efficient intermolecular energy transfer from vibrational states populated through a different VER pathway. It should be kept in mind that the excitation pulses are not monochromatic but have a spectral width of about 10 nm. Optical excitation leads to the population of several vibrational excited states, from which the energy redistribution can be expected to take different pathways.

Figure 8C shows a plot of the time constant associated with τ_{sn2} versus n_s (0−500). Although the correlation between these two quantities is not as good as that shown in Figure 8B, especially with DMSO and PrOH, a similar tendency seems to be present. This might indicate that the slower narrowing component depends mainly on the low-frequency solvent modes, while the faster component depends rather more on higher-frequency modes.

The difference in the spectral narrowing observed between Pe and PeD clearly shows that the consideration of the solvent modes alone is not sufficient to account for this process. This dissimilarity could be due to different initially populated vibrational excited states, perdeuteration leading to a lowering of all frequencies. The VER pathways in Pe and PeD might thus differ considerably and consequently the values obtained with these two chromophores cannot be readily compared. The plot of τ_{sn} with PeD in solvents where the narrowing is monophasic versus n_s (0−500) shows that the narrowing time constant decreases with increasing number of low-frequency modes in a similar fashion to the findings with Pe (Figure S3

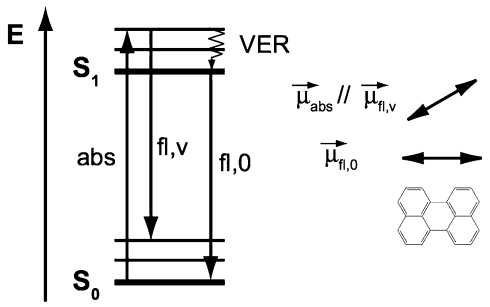

Figure 9. Energy level scheme illustrating the origin of the ultrafast decrease of fluorescence anisotropy measured at short wavelengths.

in Supporting Information). In this case as well, PrOH deviates from the correlation.

In addition, the decrease of τ_{sn1} by a factor of about 2 observed by going from ACN to ACNd agrees with an increase of n_s (0−1000) from 3 to 5. On the other hand, the τ_{sn2} values are more similar in accordance with the same n_s (0−500) for these two solvents.

The interpretation of the results is more complex with PeCN and PeOH for which dipole−dipole and H-bonding interactions are operative in polar and in protic solvents, respectively. The correlation between τ_{sn} and n_s (0−500) found with Pe and PeD can be observed with PeCN only if the values in ACN and DMSO are discarded (Figure S4 in Supporting Information). Indeed, the fast narrowing in these two solvents cannot be accounted for by their n_s (0−500) values. This discrepancy might be due to the occurrence of dipole−dipole interaction, which enhances the coupling between the polar solvent molecules and the polar PeCN.

Finally, no correlation between τ_{sn} and n_s (0−500) can be found with PeOH (Figure S5 in Supporting Information). As discussed above, this can be explained by the occurrence of H-bonding in protic solvents that accelerates VER.

Fluorescence Anisotropy. The observation of a decay component of the fluorescence anisotropy upon 400 nm excitation with a time constant similar to that of spectral narrowing also supports a scheme where intra- and intermolecular VER occur on not so largely different timescales. This ultrafast anisotropy decay that is seen on the very blue side of the fluorescence spectrum is indicative of a change of the transition responsible for the emission at this wavelength. The initial anisotropy of 0.4 suggests that emission originally takes place from the optically populated state, namely from the excited state of a Franck−Condon active vibrational mode. As the population of this state decays by both intra- and intermolecular VER, the decay time of the anisotropy is essentially the same as that of spectral narrowing. After this process, emission takes place from a lower Franck−Condon active state and, as the transition dipole differs from that involved in the excitation, the anisotropy is smaller than 0.4 (see Figure 9). The difference of anisotropy between the fluorescence from the vibrational excited state (*fl*,v) and that from the relaxed S_1 state (*fl*,0) can be explained in terms of vibrational coupling. The dipole moment for the S_0-S_1 transition of the perylenes is aligned along the long molecular axis, while those associated with the next two optical transitions are aligned along the short molecular axis.[66] Because of vibronic coupling between the S_1 and the upper excited states, the dipole moments for the vibronic S_0-S_1 transitions can be expected to have some short-axis component, the amount of which increases with the vibrational excitation. This effect has recently been reported with tetracene[67] and has also been invoked to account for the excitation wavelength dependence of initial fluorescence anisotropy of Pe.[49]

Excitation of PeCN at 400 nm leads to a vibronic transition with a dipole moment that contains some short-axis component ($\vec{\mu}_{abs}$ in Figure 9). If fluorescence takes place from this initially populated state (*fl*,v in Figure 9), the initial anisotropy should amount to 0.4, as observed here. This value drops upon VER because the transition dipole for fluorescence from the S_1 relaxed state ($\vec{\mu}_{fl,0}$) has less short-axis component. In other words, this transition dipole is no longer parallel to that responsible for absorption at 400 nm.

Summary and Conclusions

We have reported here on a detailed investigation of the influence of the solvent on the VER dynamics of perylenes after excitation with moderate excess energy by monitoring the early narrowing of the fluorescence spectrum. The results do not reveal any strong solvent dependence. No univocal effect of the strength of nonspecific solute−solvent interactions can be evidenced. On the other hand, our results point out that specific interaction such as H-bonding between solute and solvent enhance VER. Contrary to some previous investigations,[20,23] no correlation between the VER dynamics and macroscopic solvent properties, such as thermal diffusivity, can be observed here. On the other hand, a correlation with the number of low-frequency modes of the solvent molecules is found, pointing to the occurrence of V−V transfer. Moreover, other processes such as the decay of a low-frequency vibrational wavepacket and the initial decay of the fluorescence anisotropy take place on a similar time scale as spectral narrowing. All these findings are not consistent with a scheme where VER occurs in two well-separated steps, namely ultrafast sub-100 fs intramolecular vibrational redistribution and slower vibrational cooling. On the contrary, our results rather suggest that both intra- and intermolecular vibrational redistributions are closely entangled. A partial intramolecular relaxation on an ultrafast time scale is of course not ruled out, but it seems very improbable that the electronically excited molecule reaches thermal equilibrium before energy transfer to the solvent takes place. Finally, it should be noted that the experimental approach used here only gives a limited access to VER dynamics. The occurrence of VER processes slower than those found here, but which affect only weakly the fluorescence spectrum cannot be ruled out. This could explain why rather different timescales have been found for VER, depending on the experimental technique used.

It is clear that much more work is required before a clear picture of VER of large molecules in liquids is obtained.

Acknowledgment. We thank Dr. W. Fuss (MPI, Garching) for helpful discussions. We also thank the Centro Svizzero di Calcolo Scientifico (CSCS) for computational resources. This work was supported by the Fonds National Suisse de la Recherche Scientifique through project 200020-107466.

Supporting Information Available: Solvatochromic plots, plots of the spectral narrowing time constant versus the number of vibrational mode of the solvents, and calculated vibrational frequencies of the chromophores and of the solvent molecules. This material is available free of charge via the Internet at http://pubs.acs.org.

References and Notes

(1) Suppan, P. *Chemistry and Light*; RSC: Cambridge, 1994.

(2) Fuss, W.; Lochbrunner, S.; Muller, A. M.; Schikarski, T.; Schmid, W. E.; Trushin, S. A. *Chem. Phys.* **1998**, *232*, 161.

(3) Chudoba, C.; Riedle, E.; Pfeiffer, M.; Elsaesser, T. *Chem. Phys. Lett.* **1996**, *263*, 622.
(4) Lochbrunner, S.; Wurzer, A. J.; Riedle, E. *J. Chem. Phys* **2000**, *112*, 10699.
(5) Baigar, E.; Gilch, P.; Zinth, W.; Stöckl, M.; Härter, P.; von Feilitzsch, T.; Michel-Beyerle, M. E. *Chem. Phys. Lett.* **2002**, *352*, 176.
(6) Nicolet, O.; Banerji, N.; Pagès, S.; Vauthey, E. *J. Phys. Chem. A* **2005**, *109*, 8236.
(7) Madigosky, W. M.; Litovitz, T. A. *J. Chem. Phys.* **1961**, *34*, 489.
(8) Oxtoby, D. W. *Adv. Chem. Phys.* **1981**, *47*, 487.
(9) Weiner, A. M.; Ippen, E. P. *Chem. Phys. Lett.* **1985**, *114*, 456.
(10) Sukowski, U.; Seilmeier, A.; Elsaesser, T.; Fischer, S. F. *J. Chem. Phys.* **1990**, *93*, 4094.
(11) Elsaesser, T.; Kaiser, W. *Annu. Rev. Phys. Chem.* **1991**, *42*, 83.
(12) Nesbitt, D. J.; Field, R. W. *J. Phys. Chem.* **1996**, *100*, 12735.
(13) Elles, C. G.; Cox, M. J.; Crim, F. F. *J. Chem. Phys.* **2004**, *120*, 6973.
(14) Ka, B. J.; Geva, E. *J. Phys. Chem. A* **2006**, *110*, 13131.
(15) Yardley, J. T. *Introduction to Molecular Energy Transfer*; Academic Press: New York, 1980.
(16) Kovalenko, S. A.; Schanz, R.; Hennig, H.; Ernsting, N. P. *J. Chem. Phys.* **2001**, *115*, 3256.
(17) Schwarzer, D.; Hanisch, C.; Kutne, P.; Troe, J. *J. Phys. Chem. A* **2002**, *106*, 8019.
(18) Laermer, F.; Elsaesser, T.; Kaiser, W. *Chem. Phys. Lett.* **1989**, *156*, 381.
(19) Sension, R. J.; Repinec, S. T.; Hochstrasser, R. M. *J. Chem. Phys.* **1990**, *93*, 9185.
(20) Iwata, K.; Hamaguchi, H. *J. Phys. Chem. A* **1997**, *101*, 632.
(21) Pigliucci, A.; Vauthey, E. *Chimia* **2003**, *57*, 200.
(22) Iwata, K.; Hamaguchi, H. *J. Mol. Liq.* **1995**, *65*, 417.
(23) Benniston, A. C.; Matousek, P.; McCulloch, I. E.; Parker, A. W.; Towrie, M. *J. Phys. Chem. A* **2003**, *107*, 4347.
(24) Bouzou, C.; Jouvet, C.; Leblond, J. B.; Millie, P.; Tramer, A.; Sulkes, M. *Chem. Phys. Lett.* **1983**, *97*, 161.
(25) Schwartz, S. A.; Topp, M. R. *Chem. Phys.* **1984**, *86*, 245.
(26) Fourmann, B.; Jouvet, C.; Tramer, A.; Le, Bars, J. M.; Millie, P. *Chem. Phys.* **1985**, *92*, 25.
(27) Rulliere, C.; Declemy, A.; Kottis, P. *Chem. Phys. Lett.* **1984**, *110*, 308.
(28) Jiang, Y.; Blanchard, G. J. *J. Phys. Chem.* **1994**, *98*, 9411.
(29) Kiba, T.; Sato, S.-i.; Akomoto, S.; Kajasima, T.; Yamazaki, I. *J. Photochem. Photobiol., A* **2006**, *178*, 201.
(30) Hawthorne, S. B.; Miller, D. J.; Aulich, T. R. *Fresenius' J. Anal. Chem.* **1989**, *334*, 421.
(31) Buu-Hoï, N. P.; Long, C. T. *Recl. Trav. Chim. Pays-Bas* **1956**, *75*.
(32) Morandeira, A.; Engeli, L.; Vauthey, E. *J. Phys. Chem. A* **2002**, *106*, 4833.
(33) Hohenberg, P.; Kohn, W. *Phys. Rev. B* **1964**, *136*, 864.
(34) Kohn, W.; Sham, L. J. *Phys Rev. A* **1965**, *140*, 1133.
(35) Frisch, M. J.; Trucks, G. W.; Schlegel, H. B.; Scuseria, G. E.; Robb, M. A.; Cheeseman, J. R.; Montogomery Jr, J. A.; Vevren, T.; Kudin, K. N.; Burant, J. C.; Millam, J. M.; Iyengar, S. S.; Tomasi, J.; Barone, V.; Mennucci, B.; Cossi, M.; Scalmani, G.; Rega, N.; Petersson, G. A.; Nakatsuji, H.; Hada, M.; Ehara, M.; Toyota, K.; Fukuda, R.; Hasegawa, J.; Ishida, M.; Nakajima, T.; Honda, Y.; Kitao, O.; Nakai, H.; Klene, M.; Li, X.; Knox, J. E.; Hratchian, H. P.; Cross, J. B.; Bakken, V.; Adamo, C.; Jaramillo, J.; Gomperts, R.; Stratmann, R. E.; Yazyev, O.; Austin, A. J.; Cammi, R.; Pomelli, C.; Ochterski, J. W.; Ayala, P. Y.; Morokuma, K.; Voth, G. A.; Salvador, P.; Dannenberg, J. J.; Zakrzewski, V. G.; Dapprich, S.; Daniels, A. D.; Strain, M. C.; Farkas, O.; Malick, D. K.; Rabuck, A. D.; Raghavachari, K.; Foresman, J. B.; Ortiz, J. V.; Cui, Q.; Baboul, A. G.; Clifford, S.; Ciolowski, J.; Stefanov, B. B.; Liu, G.; Liashenko, A.; Piskorz, P.; Komaromi, I.; Martin, R. L.; Keith, T.; Al-Laham, M. A.; Peng, C. Y.; Nanayakkara, A.; Challacombe, M.; Gill, P. M. W.; Johnson, B.; Chen, W.; Wong, M. W.; Gonzalez, C.; Pople, J. A. *Gaussian 03*, revision D.01; Gaussian, Inc.: Wallingford, CT, 2004.
(36) Perdew, J. P.; Burke, K.; Ernzerhof, M. *Phys. Rev. Lett.* **1996**, *77*, 3865.
(37) Krishnan, R.; Binkley, J. S.; Seeger, R.; Pople, J. A. *J. Chem. Phys.* **1980**, *72*, 650.
(38) Clark, T.; Chandrasekhar, J.; Schleyer, P. v. R. *J. Comput. Chem.* **1983**, *4*, 294.
(39) Suppan, P. *J. Photochem. Photobiol.* **1990**, *A50*, 293.
(40) Morandeira, A.; Fürstenberg, A.; Gumy, J.-C.; Vauthey, E. *J. Phys. Chem. A* **2003**, *107*, 5375.
(41) Schwarzer, D.; Kutne, P.; Schröder, C.; Troe, J. *J. Chem. Phys.* **2004**, *121*, 1754.
(42) Horng, M. L.; Gardecki, J. A.; Papazyan, A.; Maroncelli, M. *J. Phys. Chem.* **1995**, *99*, 17311.
(43) Cave, R. J.; Castner, E. W., Jr. *J. Phys. Chem. A* **2002**, *106*, 12117.
(44) Arzhantsev, S.; Zachariasse, K. A.; Maroncelli, M. *J. Phys. Chem. A* **2006**, *110*, 3454.
(45) Christensen, R. L.; Drake, R. C.; Phillips, D. *J. Phys. Chem.* **1986**, *90*, 5960.
(46) Kalman, B.; Clarke, N.; Johansson, L. B.-Å. *J. Phys. Chem.* **1989**, *93*, 4608.
(47) Brocklehurst, B.; Young, R. N. *J. Phys. Chem.* **1995**, *99*, 40.
(48) Goldie, S. N.; Blanchard, G. J. *J. Phys. Chem. A* **1999**, *103*, 999.
(49) Piston, D. W.; Bilash, T.; Gratton, E. *J. Phys. Chem.* **1989**, *93*, 3963.
(50) Hill, T. L. *An Introduction to Statistical Thermodynamics*; Dover: New York, 1986.
(51) Ong, K. K.; Jensen, J. O.; Hameka, H. F. *J. Mol. Struct.* **1999**, *459*, 131.
(52) Tan, X.; Salama, F. *J. Chem. Phys.* **2005**, *122*, 084318.
(53) Brodard, P.; Vauthey, E. *J. Phys. Chem. B* **2005**, *109*, 4668.
(54) Mohamed, M. B.; Ahmadi, T. S.; Link, S.; Braun, M.; El-Sayed, M. A. *Chem. Phys. Lett.* **2001**, *343*, 55.
(55) Miranda, L. C. M.; Cella, N. *Phys. Rev. B* **1993**, *47*, 3896.
(56) Watanabe, H.; Kato, H. *J. Chem. Eng. Data* **2004**, *49*, 809.
(57) Siemiarczuk, A.; Wagner, B. D.; Ware, W. R. *J. Phys. Chem.* **1990**, *94*, 1661.
(58) Wlodarczyk, J.; Kierdaszuk, B. *Biophys. J.* **2003**, *85*, 589.
(59) Suppan, P.; Ghoneim, N. *Solvatochromism*; The Royal Society of Chemistry: Cambridge, 1997.
(60) Sulkes, M. *Chem. Phys.* **1987**, *114*, 289.
(61) Remmers, K.; Meerts, W. L.; Zehnacker-Rentien, A.; Le, Barbu, K.; Lahmani, F. *J. Chem. Phys.* **2000**, *112*, 6237.
(62) Yatsuhashi, T.; Trushin, S. A.; Fuss, W.; Rettig, W.; Schmid, W. E.; Zilberg, S. *Chem. Phys.* **2004**, *296*, 1.
(63) Amirav, A.; Even, U.; Jortner, J. *Chem. Phys. Lett.* **1980**, *72*, 21.
(64) Fillaux, F. *Chem. Phys. Lett.* **1985**, *114*, 384.
(65) Joblin, C.; Salama, F.; Allamandola, L. *J. Chem. Phys.* **1995**, *102*, 9743.
(66) Fuke, K.; Kaya, K.; Kajiwara, T.; Nagakura, S. *J. Mol. Spectrosc.* **1976**, *63*, 98.
(67) Sarkar, N.; Takeuchi, S.; Tahara, T. *J. Phys. Chem.* **1999**, *103*, 4808.